SCIENTIFIC REPORTS

OPEN

SUBJECT AREAS:
METALS AND ALLOYS
GLASSES
STRUCTURE OF SOLIDS AND LIQUIDS
MECHANICAL ENGINEERING

Received
24 June 2013

Accepted
25 March 2014

Published
11 April 2014

Correspondence and requests for materials should be addressed to Q.W. (qingwang@shu.edu.cn); Y.Y. (yonyang@cityu.edu.hk) or J.L. (jianlu@cityu.edu.hk)

The atomic-scale mechanism for the enhanced glass-forming-ability of a Cu-Zr based bulk metallic glass with minor element additions

Q. Wang[1,2], C. T. Liu[2], Y. Yang[2], J. B. Liu[2], Y. D. Dong[1] & J. Lu[2,3]

[1]Key laboratory for structures, Institute of materials science, Shanghai University, Shanghai, China, [2]Department of Mechanical and Biomedical Engineering, City University of Hong Kong, Kowloon, Hong Kong, China, [3]Centre for Advanced Structural Materials, Shenzhen Research Institute, City University of Hong Kong, 8 Yuexing 1st Road, Shenzhen Hi-Tech Industrial Park, Nanshan District, Shenzhen, China.

It is known that the glass forming-ability (GFA) of bulk metallic glasses (BMGs) can be greatly enhanced via minor element additions. However, direct evidence has been lacking to reveal its structural origin despite different theories hitherto proposed. Through the high-resolution transmission-electron-microscopy (HRTEM) analysis, here we show that the content of local crystal-like orders increases significantly in a Cu-Zr-Al BMG after a 2-at% Y addition. Contrasting the previous studies, our current results indicate that the formation of crystal-like order at the atomic scale plays an important role in enhancing the GFA of the Cu-Zr-Al base BMG.

Minor element additions (or micro-alloying) have been widely used in the metallurgical fields, which are also known as an effective means to improve the glass forming ability (GFA) of various glass-forming liquids[1–7]. For instance, the critical diameter of Cu-Zr-Al metallic glass rods is known to be ~3 mm; however, it can be increased to 8 mm after adding only 2–5 at.% of Y to the glass-forming system[5]. Although further addition of Y could be detrimental and reduce the GFA, however, the beneficial effect of micro-alloying has been well recognized and exploited in the casting of various bulk metallic glasses (BMGs)[5–9].

To rationalize the micro-alloying effect, different theories were put forward. For example, it was proposed that micro-alloying could scavenge oxygen impurities and thus suppress the heterogeneous nucleation of crystals in supercooled liquids[5,8,9]; or that it could tailor the composition of the system in such a way that the resultant structure could approach to a deep eutectic composition, therefore stabilizing the liquid phase[5], Furthermore, it was even argued that micro-alloying can introduce an atomic-level strain energy into the glass-forming liquid so that the thermodynamic driving force for crystal precipitation is impaired[7]. In spite of all these theories, the structural origin of the micro-alloying effect is still elusive, particularly, at the atomic scale.

Over the past years, the atomic structure of metallic glass-forming liquids and glasses has received intensive research efforts, the focus of which has been centered on the understanding of the ordered phase, such as the short- and medium-range order, in an amorphous structures[10–26]. In general, it has been shown that the ordered atomic clusters with either local icosahedral-like[14–20] or crystal-like[11–13] symmetry are of great importance to the vitrification behavior of metallic glass-forming liquids[25,27–29]. Therefore, it is natural to ask whether micro-alloying could possibly affect these atomic clusters in altering the GFA of a given BMG. The answer to the question may further our understanding of the structural origin of the micro-alloying effect, which sets the goal of our current research.

Results

Figures 1(a)–(b) display the HRTEM images of the as-cast $Cu_{46}Zr_{47-x}Al_7Y_x$ (x = 0, 2) BMGs. At a first glance, both amorphous structures look similar and exhibit a maze-like pattern. There is no overall crystallization as seen in the HRTEM images, which is consistent with the XRD results (see Supplementary Materials). However, it is worthy of mentioning that the selected area electron diffraction (SAED) pattern (inset of Fig. 1b) obtained from the Y-containing BMG shows a halo ring slightly thinner than that of the Y-free BMG (inset of Fig. 1a), implying

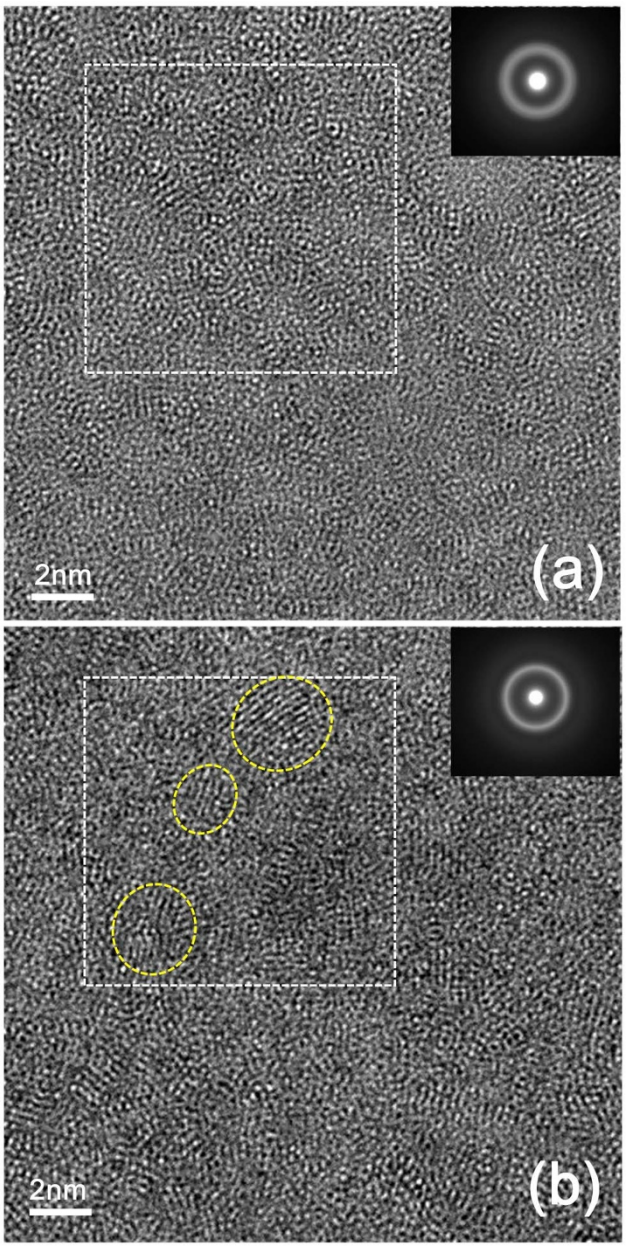

Figure 1 | The HRTEM images for the as-cast $Cu_{46}Zr_{47}Al_7$ (a) and $Cu_{46}Zr_{45}Al_7Y_2$ (b) BMGs (inset: the selected area diffraction pattern).

that there might be an increasing degree of structural ordering, although still in an overall amorphous state, after the minor substitution of Zr with Y element in the Cu-Zr-Al BMG.

Such micro-alloying induced structural ordering could be further examined on the Fast-Fourier-Transformation (FFT) filtered HRTEM images. Figures 2a and b show the FFT-filtered images of the selected rectangular areas in Figs. 1a–b (dashed line), respectively. As seen in these FFT-filtered images (Figs. 2a–b), both samples contain crystal-like (marked by the yellow rectangles) atomic clusters, which are typically of 1–2 nm in size and characterized by a local fringe pattern reminiscence of a translational symmetry. Note that similar ordered atomic structures have been identified by using HRTEM in various metallic glasses[12,13,30,31].

Despite the presence of the crystal-like order on the scale of 1–2 nm, the structural amorphousness is still retained. The inset of Fig. 2a shows the diffraction pattern of the region with crystal-like order in the Y-free sample, which displays no diffraction spots but an amorphous halo ring. Apparently, there is a trend that the crystal-like orders grow with the Y addition. As shown in the inset of Fig. 2b, one can clearly see crystal-like-order regions of ~2–4 nm in size, which corresponds to three pairs of diffraction spots. As compared to fully crystallized regions, which are associated with a 3D translational symmetry, these regions with an imperfect translational order are usually interpreted as the crystalline nuclei, which has been observed during crystallization in other types of BMGs[31] and proteins[32]. Indeed, the growth of the crystal-like order is evident at many places in the Y-containing BMG; however, the size of all growing crystal-like orders is limited within the range of 2–4 nm, which is insufficient to change the overall structural amorphousness. The limited growth of the local crystal-like orders, as apparently induced by micro-alloying, could be attributed to the introduction of the atomic-level strain energy into Gibbs free energy for crystal nucleation[7] and/or presence of the icosahedral-like clusters, which circle around the crystal-like-order regions and act like pinning 'particles' to suppress large-scale crystallization, as discussed in the recent work[33]. Moreover, as shown in table 1, the nanobeam EDS analysis reveals that the selected area with crystal-like atomic clusters of about 4 nm contains Y element and is enriched in Cu element; in contrast their surroundings free of Y is poor in Cu but enriched in Zr. Considering the positive enthalpy of mixing (+35 kJ/mol) between Y and Zr, the local variation in composition can be attributed to the partial substitution of Zr with Y. Therefore, we believe that the emergence of the crystal-like orders is spatially associated with the added Y element, leading to local chemical fluctuations that stabilize the Y-containing supercooled liquid. Note that for this family of Cu-Zr based BMGs the primary crystallization phases have been identified to be CuZr or $Cu_{10}Zr_7$[7], of

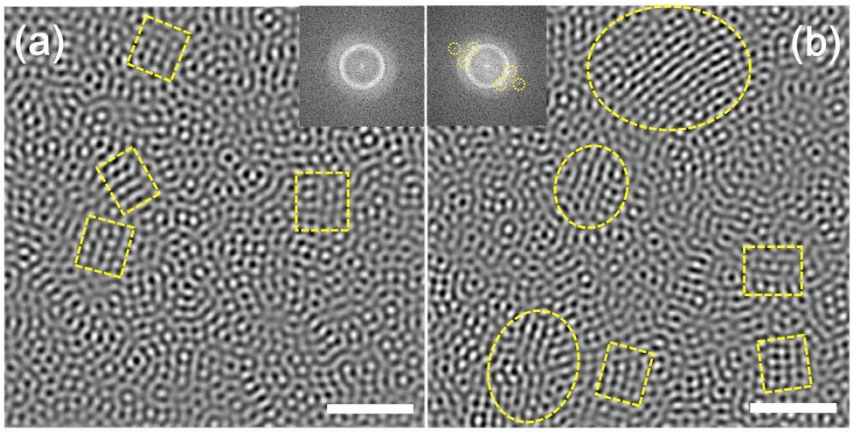

Figure 2 | Typical localized crystal-like atomic ordering observed in the as-cast $Cu_{46}Zr_{47-x}Al_7Y_x$ (x = 0, 2) BMG alloys. (a) and (b) are the FFT-filtered images of the areas selected from Figs. 1 (a) and (b) (indicated by the dashed box), respectively, showing the atomic configurations for an amorphous region with ordered clusters. Insets show the corresponding diffraction patterns of (a–b) obtained via FFT. (scale bar = 2 nm).

Table 1 | The EDS results obtained for the $Cu_{46}Zr_{47}Al_7Y_2$ BMG alloy. Notes: A1 stands for the selected areas containing a crystal-like order (CLO) at nanoscale of about 4 nm, and A2 for their nearby areas without CLO

	Cu (at%)	Zr (at%)	Al (at%)	Y (at%)
A1	55.2 ± 3.4	37.3 ± 2.2	6.2 ± 1.2	1.4 ± 0.1
A2	22.6 ± 2.0	62.8 ± 6.1	14.7 ± 4.1	

which the compositions are different from those of the areas containing crystal-like atomic clusters.

To quantify the areal fraction of local crystal-like order, our obtained HRTEM images, such as those shown in Figs. 1a–b, are divided into many square cells (Fig. 3). Each cell spans a size of 1.915 nm, close to the smallest size of the observed crystal-like order, and subsequently the image in each cell is transformed into its 2D auto-correlation map in order to assess the local translational symmetry[31,34,35]. For instance, the cell located in the 1st row and 4th column in Fig. 3 is characterized by crystal-like symmetry in its Fast Fourier Transformation (FFT) pattern (not shown here) and exhibits fringes in the 2D auto-correlation map. Therefore, it was chosen as a reference pattern to study the local ordering in the present case. In that regard, all the sub-images in the rest of square cells were considered to be ordered if their 2D auto-correlation patterns display a clearer fringe than the reference one.

Following the above method, we analyzed all cells in the HRTEM images. Our results show that the total areal fraction of the crystal-like-order regions is 24.5 ± 1.5% in the Y-free sample, which agrees with the previous estimation made on the Zr-based BMG (Vit1) using the same method[31]. By comparison, the areal fraction increases to 36 ± 2% in the Y-containing sample (see Fig. 7S in Supplementary Information), indicating the enhanced structural ordering as one could also infer from the SAED pattern previously shown (the inset of Fig. 1b). It should be noted that the crystal-like structures marked in the HRTEM image with dashed yellow lines exhibit a distinct crystalline diffraction in the corresponding FFT and always yield the crystal-like auto-correlation pattern, as shown in Fig. 8S. However, there are also places which show the crystal-like auto-correlation pattern and diffraction spots in FFT even though they do not exhibit prominent crystal-like order in the HRTEM image (see Fig. 8S). In line with the auto-correlation method, we counted both places as those with local crystal-like order.

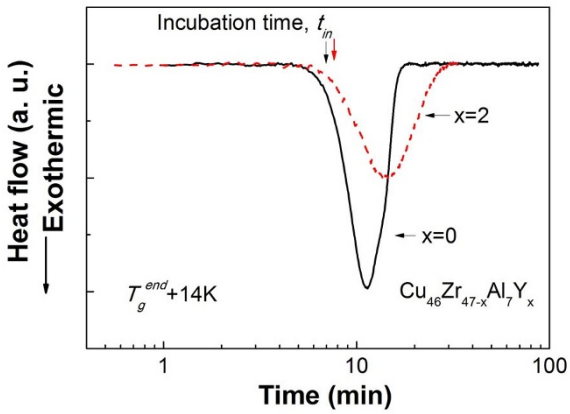

Figure 4 | Isothermal DSC traces for $Cu_{46}Zr_{47-x}Al_7Y_x$(x = 0, 2) held in supercooled liquid region at T_g^{end} + 14K.

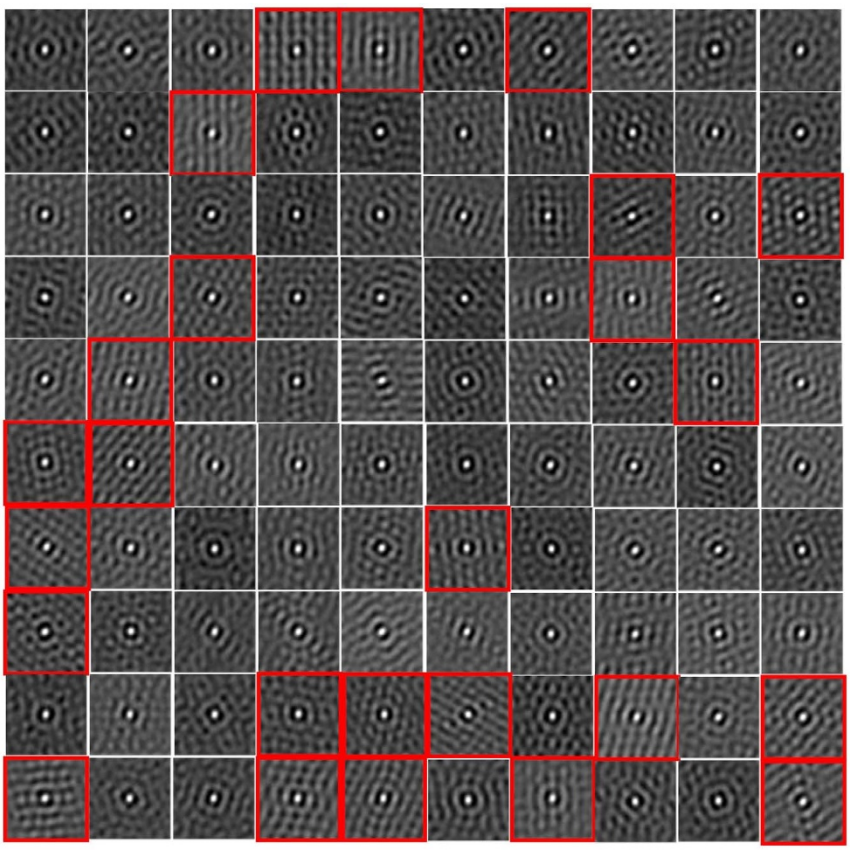

Figure 3 | The segmentation of the HRTEM image for the $Cu_{46}Zr_{47}Al_7$ BMG for auto-correlation analysis. The dimension of each segment or cell is 1.915 × 1.915 nm^2.

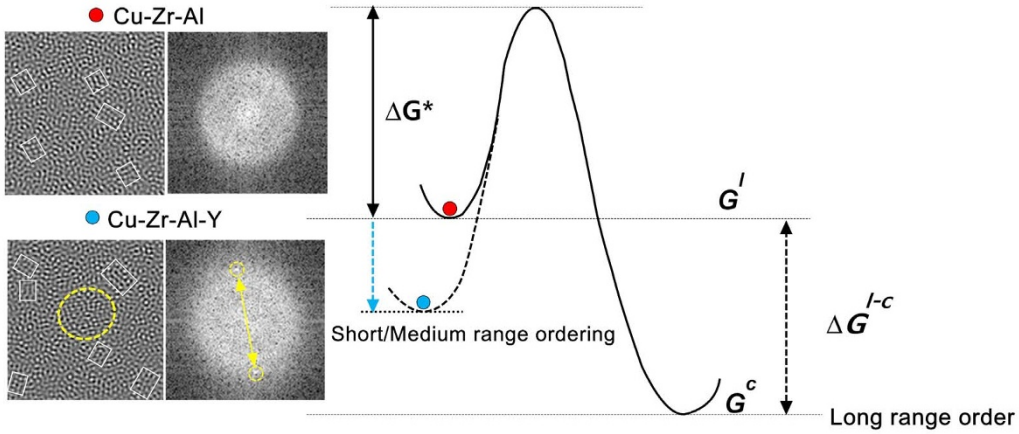

Figure 5 | The schematics of the free energy profiles for the $Cu_{46}Zr_{47-x}Al_7Y_x$ (x = 0, 2) BMG forming supercooled liquids showing the effect of structural ordering due to the minor Y element addition.

To bridge the observed atomic structure features and the macroscopic thermodynamics, we examined the crystallization behavior of $Cu_{46}Zr_{47-x}Al_7Y_x$ (x = 0, 2) by using DSC. According to Chen and Spaepen[36], isothermal calorimetry is able to distinguish a glassy structure from that containing nano-grains. For the as-cast $Cu_{46}Zr_{47-x}Al_7Y_x$(x = 0, 2), the clear exothermic peak in the isothermal DSC traces, as shown in Fig. 4, clearly indicates their glassy nature, contrasting the decaying exothermic signal expected for the coarsening of a ultra-fine-grained polycrystalline structure[36]. In addition, the amorphous nature of both alloys is also confirmed by the distinct glass transition and sharp crystallization peak (see Fig. 2S). More interestingly, it should be noted that, after the minor addition of the 2 at % Y, the isothermal exothermic crystallization reaction is significantly delayed, as indicated by the increased incubation time. Furthermore, strain rate jump compression tests were also performed at various temperatures to obtain the rheological properties of the Cu-Zr based BMG alloys in the supercooled liquid regions (see Supplementary Information for details). As shown in Fig. 3S, adding the 2 at % Y brings about a distinct increase in the viscosity of the supercooled liquid, echoing the emergence of more atomic clusters of crystal-like order, as shown in Figs. 1 and 2.

Discussion

The above experimental results clearly show that, after the increasing content of crystal-like orders with the Y addition, the overall rate of crystallization is reduced. This behavior is in line with the enhanced GFA of the BMG but brings about a seeming paradox, i.e. why the increasing degree of crystal-like order, usually interpreted as crystallization nuclei, does not accelerate the overall crystallization rate in the glass-forming liquid. To explain this, one may note the competition between the growth of crystal- and icosahedra-like orders, taking into account that previous investigations have indicated their co-existence in the Cu-Zr based BMG alloy[14]. As the atomic ordering with a spherical-like symmetry maximizes local atomic densities and is usually favored over the latter during an ordering process of a glass-forming liquid[28], these icosahedra-like clusters could pin the boundary of the crystal-like clusters later formed and thus constraint their growth, as discussed in Ref. 33.

As a whole, as long as the Y concentration is low and thus the pinning effect is still operative, the whole supercooled liquids would remain in their amorphous state. Once the growth of the local crystal-like order is constrained, the increased overall structural ordering reduces the thermodynamic driving force for crystallization. As illustrated in Fig. 5, the free-energy of the metallic glass-forming liquid is lowered down as a result of the structural ordering due to micro-alloying. Following the classic thermodynamics, the free-energy difference, ΔG^{l-c}, between the liquid and crystalline phase decreases. According to Ref. 37, the free energy barrier ΔG^* against crystallization can be expressed as $\Delta G^* = 16\pi\gamma_{l-c}^3/3(\Delta G^{l-c})^2$, in which γ_{l-c} denotes the interface tension between the liquid and crystal. Obviously, ΔG^* increases with the decreasing ΔG^{l-c} for a given γ_{l-c}. Since the crystallization rate is given by $I = \frac{k_n}{\eta}\exp(-\Delta G^*/k_BT)$, where k_n is a constant, η the viscosity, k_B the Boltzmann constant, and T the temperature, the crystallization rate I becomes slow down because of the micro-alloying induced structural ordering, which then leads to an enhanced GFA.

To sum up, our experimental results clearly show that the minor addition of Y results in formation of more crystal-like orders. These regions of crystal-like order, emerging at a low Y concentration, cannot grow to alter the overall structural amorphousness; however, this micro-alloying induced structural ordering effectively increases the viscosity of the super cooled liquid and reduces the thermodynamic driving force for crystallization, leading to the slow-down of the crystallization rate and hence the enhanced GFA of the glass-forming liquid.

Methods

In this work, the Cu-Zr-Al metallic-glass forming liquid was chosen as the model material. To study the micro-alloying effect, the multicomponent $Cu_{46}Zr_{47-x}Al_7Y_x$ (x = 0, 2) BMG cylindrical rods of 3 mm diameter were prepared by copper mold suction casting in a Ti-gettered high-purity argon atmosphere. The amorphous structures of the as-cast samples were characterized with X-ray diffraction (XRD) using Co Kα radiation and differential scanning calorimetry (DSC) under a flow of purified argon in a Perkin-Elmer DSC7 (see supplementary materials for detail). Subsequently, extensive structural analyses on the as-cast samples were performed using the high resolution transmission electron microscopy (HRTEM) with an accelerating voltage of 200 kV (JEOL 2010F and Philips CM200). For our study, reliable HRTEM images were obtained by varying the defocus until an optimum condition was found (see Supplementary Materials). To quantitatively study the atomic-scale structural ordering, the HRTEM images were transformed to their corresponding autocorrelation patterns by following the method well established in literature[34,35,38,39] Chemical compositions were analyzed by using nano-beam energy dispersive spectrometry (EDS) linked with TEM. Note that a great care was taken during the preparation of the TEM samples, which underwent several steps from the initial mechanical thinning to the thickness of ~80 μm, and the subsequent standard twin-jet electrochemical thinning using a HClO4–C2H5OH solution (volume ratio: 1 : 10) at about 248 K, and finally to low-angle ion milling for ~10 min until the resultant sample thickness was estimated less than ~20 nm. To measure the local thickness of the TEM specimens, the method based on the electron energy loss spectroscopy (EELS) was employed (See Supplementary Information for details).

1. Wang, W. H. Roles of minor additions in formation and properties of bulk metallic glasses. *Prog. Mater. Sci.* **52**, 540–596 (2007).
2. Liu, C. T. & Lu, Z. P. Effect of minor alloying additions on glass formation in bulk metallic glasses. *Intermetallics* **13**, 415–418 (2005).
3. Cheng, Y. Q., Ma, E. & Sheng, H. W. Alloying strongly influences the structure, dynamics, and glass forming ability of metallic supercooled liquids. *Appl. Phys. Lett.* **93**, 111913 (2008).

4. Chen, N., Martin, L., Luzguine-Luzgin, D. V. & Inoue, A. Role of Alloying Additions in Glass Formation and Properties of Bulk Metallic Glasses. *Materials* **3**, 5320–5339 (2010).
5. Xu, D. H., Duan, G. & Johnson, W. L. Unusual Glass-Forming Ability of Bulk Amorphous Alloys Based on Ordinary Metal Copper. *Phys. Rev. Lett.* **92**, 245504 (2004).
6. Park, E. & Kim, D. Phase separation and enhancement of plasticity in Cu–Zr–Al–Y bulk metallic glasses. *Acta Mater.* **54**, 2597–2604 (2006).
7. Zhang, Y., Chen, J., Chen, G. L. & Liu, X. J. Glass formation mechanism of minor yttrium addition in CuZrAl alloys. *Appl. Phys. Lett.* **89**, 131904 (2006).
8. Zhang, Y., Pan, M. X., Zhao, D. Q., Wang, R. J. & Wang, W. H. Formation of Zr-based bulk metallic glasses from low purity of materials by Yttrium addition. *Mater. Tran., JIM* **41**, 1410–1414 (2000).
9. Lu, Z., Liu, C., Thompson, J. & Porter, W. Structural Amorphous Steels. *Phys. Rev. Lett.* **92**, 245503 (2004).
10. Hirata, A. *et al.* Direct observation of local atomic order in a metallic glass. *Nat. Mater.* **10**, 28–33 (2010).
11. Hwang, J. *et al.* Nanoscale Structure and Structural Relaxation in $Zr_{50}Cu_{45}Al_5$ Bulk Metallic Glass. *Phys. Rev. Lett.* **108**, 195505 (2012).
12. Hirata, A., Hirotsu, Y., Ohkubo, T., Tanaka, N. & Nieh, T. G. Local atomic structure of Pd–Ni–P bulk metallic glass examined by high-resolution electron microscopy and electron diffraction. *Intermetallics* **14**, 903–907 (2006).
13. Hirotsu, Y., Nieh, T., Hirata, A., Ohkubo, T. & Tanaka, N. Local atomic ordering and nanoscale phase separation in a Pd-Ni-P bulk metallic glass. *Phys. Rev. B* **73**, 012205 (2006).
14. Cheng, Y., Ma, E. & Sheng, H. Atomic Level Structure in Multicomponent Bulk Metallic Glass. *Phys. Rev. Lett.* **102**, 245501 (2009).
15. Cozzini, S. & Ronchetti, M. Local icosahedral structures in binary-alloy clusters from molecular-dynamics simulation. *Phys. Rev. B* **53**, 12040–12049 (1996).
16. Saida, J., Matsushita, M. & Inoue, A. Direct observation of icosahedral cluster in $Zr_{70}Pd_{30}$ binary glassy alloy. *Appl. Phys. Lett.* **79**, 412–414 (2001).
17. Takagi, T. *et al.* Local structure of amorphous $Zr_{70}Pd_{30}$ alloy studied by electron diffraction. *Appl. Phys. Lett.* **79**, 485–487 (2001).
18. Saksl, K. *et al.* Evidence of icosahedral short-range order in $Zr_{70}Cu_{30}$ and $Zr_{70}Cu_{29}Pd_1$ metallic glasses. *Appl. Phys. Lett.* **83**, 3924–3926 (2003).
19. Luo, W. *et al.* Icosahedral Short-Range Order in Amorphous Alloys. *Phys. Rev. Lett.* **92**, 145502 (2004).
20. Fujita, T. *et al.* Atomic-Scale Heterogeneity of a Multicomponent Bulk Metallic Glass with Excellent Glass Forming Ability. *Phys. Rev. Lett.* **103**, 075502 (2009).
21. Cheng, Y. Q. & Ma, E. Atomic-level structure and structure–property relationship in metallic glasses. *Prog. Mater. Sci.* **56**, 379–473 (2011).
22. Xing, L. Q., Hufnagel, T. C., Eckert, J., Loser, W. & Schultz, L. Relation between short-range order and crystallization behavior in Zr-based amorphous alloys. *Appl. Phys. Lett.* **77**, 1970–1972 (2000).
23. Sheng, H. W. *et al.* Polyamorphism in a metallic glass. *Nat. Mater.* **6**, 192–197 (2007).
24. Sheng, H. W., Luo, W. K., Alamgir, F. M., Bai, J. M. & Ma, E. Atomic packing and short-to-medium-range order in metallic glasses. *Nature* **439**, 419–425 (2006).
25. Jakse, N. & Pasturel, A. Glass forming ability and short-range order in a binary bulk metallic glass by ab initio molecular dynamics. *Appl. Phys. Lett.* **93**, 113104 (2008).
26. Ye, J. C., Lu, J., Liu, T. C., Wang, Q. & Yang, Y. Atomistic free-volume zones and inelastic deformation of metallic glasses. *Nat. Mater.* **9**, 619–623 (2010).
27. Shintani, H. & Tanaka, H. Frustration on the way to crystallization in glass. *Nat. Phys.* **2**, 200–206 (2006).
28. Leocmach, M. & Tanaka, H. Roles of icosahedral and crystal-like order in the hard spheres glass transition. *Nat. Commun.* **3**, 974 (2012).
29. Takeshi, K. & Tanaka, H. Formation of a crystal nucleus from liquid. *Proc. Nat. Acad. Sci.* **107**, 14036–14041 (2010).
30. Liu, X. J. *et al.* Growth mechanism from nano-ordered clusters to nanocrystals in a deeply undercooled melt of Zr-Ni-Ti metallic glass. *J. Appl. Phys.* **102**, 063515 (2007).
31. Liu, X. J. *et al.* Atomistic mechanism for nanocrystallization of metallic glasses. *Acta Mater.* **56**, 2760–2769 (2008).
32. Yau, S.-T. & Vekilov, P. G. Quasi-planar nucleus structure in apoferritin crystallization. *Nature* **406**, 494–497 (2000).
33. Wang, Q., Liu, C. T., Yang, Y., Dong, Y. D. & Lu, J. Atomic-Scale Structural Evolution and Stability of Supercooled Liquid of a Zr-Based Bulk Metallic Glass. *Phys. Rev. Lett.* **106**, 215505 (2011).
34. Fan, G. Y. & Cowley, J. M. Auto-correlation analyssi of high resolution electron micrographs of near-amorphous thin films. *Ultramicroscopy* **17**, 345–356 (1985).
35. Liang, J. M. & Chen, L. J. Autocorrelation of interfacial function analysis of phase formation in the initial stage reactions of molybdenum thin films on (1ll) Si. *Appl. Phys. Lett.* **64**, 1224–1226 (1994).
36. Chen, L. C. & Spaepen, F. Calorimetric evidence for the micro-quasicrystalline structure of 'amorphous' Al/transition metal alloys. *Nature* **336**, 366–368 (1988).
37. Turnbull, D. Under what conditions can a glass be formed? *Contemp Phys* **10**, 473–488 (1969).
38. Chang, S. M., Huang, H. Y., Yang, H. Y. & Chen, L. J. Mechanism of enhanced formation of C54–TiSi2 in high-temperature deposited Ti thin films on preamorphized (001)Si. *Appl. Phys. Lett.* **74**, 224 (1999).
39. Cheng, S. L. *et al.* Evolution of structural order in germanium ion-implanted amorphous silicon layers. *J. Appl. Phys.* **92**, 910 (2002).

Acknowledgments

Q.W. would like to acknowledge the financial supports provided by Natural Science Foundation of China (Grant No. 50871063, 51171099) and from the 085 project in Shanghai University. The research of YY is supported by the Research Grant Council (RGC) of the Hong Kong government through the General Research Fund (GRF) with the grant number CityU 530711, and the research of CTL is supported by the Hong Kong RGC with Grant No. CityU 522110. J.L. acknowledges the financial support provided by the Grant 2012CB932203 of the National Key Basic Research Program of the Chinese Ministry of Science and Technology.

Author contributions

Q.W. and J.B.L. carried out the experiments. Q.W., Y.Y. and C.T.L. analyzed the data. J.L., Q.W., C.T.L., Y.D.Y. and Y.Y. contributed to the discussion of the results. Y.Y. and Q.W. wrote the manuscript.

Additional information

Supplementary information accompanies this paper at http://www.nature.com/scientificreports

Competing financial interests: The authors declare no competing financial interests.

How to cite this article: Wang, Q. et al. The atomic-scale mechanism for the enhanced glass-forming-ability of a Cu-Zr based bulk metallic glass with minor element additions. *Sci. Rep.* **4**, 4648; DOI:10.1038/srep04648 (2014).